Depletion interaction of casein micelles and an exocellular polysaccharide

Depletion interaction of casein micelles and an exocellular polysaccharide

R. Tuinier,[1,2] E. ten Grotenhuis,[1] C. Holt,[3] P. A. Timmins,[4] and C. G. de Kruif[1,*]
[1]*NIZO Food Research, P.O. Box 20, 6710 BA Ede, The Netherlands*
[2]*Laboratory of Physical Chemistry and Colloid Science, Wageningen University, Dreijenplein 6, 6703 HB Wageningen, The Netherlands*
[3]*Hannah Research Institute, Ayr KA6 5HL, Scotland, United Kingdom*
[4]*Institut Max von Laue–Paul Langevin, Avenue des Martyrs, Boîte Postale 156 F-38042, Grenoble, France*
(Received 19 November 1998)

Casein micelles become mutually attractive when an exocellular polysaccharide produced by *Lactococcus lactis* subsp. *cremoris* NIZO B40 (hereafter called EPS) is added to skim milk. The attraction can be explained as a depletion interaction between the casein micelles induced by the nonadsorbing EPS. We used three scattering techniques (small-angle neutron scattering, turbidity measurements, and dynamic light scattering) to measure the attraction. In order to connect the theory of depletion interaction with experiment, we calculated structure factors of hard spheres interacting by a depletion pair potential. Theoretical predictions and all the experiments showed that casein micelles became more attractive upon increasing the EPS concentration. [S1063-651X(99)11307-2]

PACS number(s): 87.14.−g, 82.70.Dd

I. INTRODUCTION

There is a significant interest in the production of exocellular polysaccharides (EPS's) by food grade microorganisms [1]. A familiar example is the *in situ* production of EPS's by lactic acid bacteria in products such as yogurt and viilli [2]. The EPS seems to influence the rheological properties of these products, and is responsible for the threadlike pouring behavior which is also referred to as ''long behavior'' (see van Marle [3]).

Much attention has been given to the analysis of the chemical structure of the monomeric units of EPS's [4–6]. Previously, we characterized various properties of an EPS produced by *Lactococcus lactis* subsp. *cremoris* strain NIZO B40 [7]. This EPS has a number-averaged molar mass (M_n) of 1.47×10^6 g/mol, a number-averaged radius of gyration of 86 nm [7], and a polydispersity index M_w/M_n of 1.13; here M_w is the weight-averaged molar mass. This polysaccharide has interesting thickening capacities in comparison with other polysaccharides, and is a common ingredient of ''health foods.''

In a dairy product like yogurt containing both polysaccharides and proteins, both biopolymers contribute to the structural and textural properties of food products by their thickening properties, gel formation, and water-binding capacity. When there are significant interactions between polysaccharide and protein, the ternary mixture is not ideal [8].

Therefore we have studied the effect of added EPS on the physical properties of a (model) dairy product. As a model system we chose low-heat skim milk, prepared from reconstituted skim milk powder, since this protein dispersion is simpler than commercial dairy products. From a colloid physics point of view skim milk can be considered as a dispersion of casein micelles (about 100-nm radius and a volume fraction $\phi\approx0.1$) in a continuous phase containing water, salts, lactose and small (<5 nm) globular proteins. Previous work has shown that casein micelles in such a system behave effectively as hard spheres [9].

From previous work [8,10,11] it follows that incompatibility is a general phenomenon in protein-polysaccharide solutions. This originates from the fact that saccharide-amino acid contacts are usually energetically unfavorable compared with the interaction with the solvent [8]. A repulsive polysaccharide-protein interaction leads to an attractive interaction between the globular proteins commonly refferred to as depletion interaction. In the case of protein particles, such as casein micelles in milk, a depletion layer is present when a polysaccharide does not adsorb onto the casein micelle. The physics of depletion interactions can be understood as follows. On mixing colloidal particles with swollen polymer molecules, the centers of mass of these molecules are excluded from a zone of liquid adjacent to the surface of the rigid object. This zone has a thickness equal to an average effective radius of the polymer molecule. In the depletion layer the osmotic pressure (Π_p) due to the polymer is smaller than in the bulk due to a lower polymer segment concentration in that layer. Brownian motion of the casein micelles occasionally causes overlap of two depletion layers. This overlap volume (V_{overlap}) of two depleted layers increases the bulk volume available to the polymer and thereby decreases the free energy of the system by an amount $\Pi_p V_{\mathrm{overlap}}$. The result is that the colloidal particles tend to stick together. One may say they are pushed together by the unbalanced osmotic pressure difference. Asakura and Oosawa [12] were the first to describe the origin of the depletion interaction between colloidal particles and nonadsorbing polymers. They pointed out that the attractive force between the particles is proportional to the osmotic pressure of the polymer solution.

Upon increasing the attraction between the particles, a phase separation into a colloidal gas and a colloidal liquid phase may occur [13,14]. Making colloidal particles attrac-

*Author to whom correspondence should be addressed. Electronic address: dekruif@nizo.nl

tive does not only change the phase behavior but also affects transport properties such as diffusion, sedimentation, and rheology of the suspension [15].

We have used various scattering methods in order to determine the strength of the attractions between the casein micelles in the presence of an EPS. In Sec. II we first discuss theoretical approaches which were used to interpret the experimental results. The materials and experimental techniques used are explained in Sec. III. We present the results in Sec. IV.

II. THEORY

A. Depletion interaction theory

Vrij [16] developed a theory which allows a calculation of the attractive potential between two hard spheres as induced by the presence of nonadsorbing polymer molecules. The polymer molecules, with an effective diameter σ_p (twice the depletion layer thickness Δ) are mutually freely permeable (θ solvent) but are hard spheres for the colloids. The approach of Vrij is only valid for polymer molecules which are smaller than the colloidal spheres, since it is tacitly assumed that the center of mass of a polymer molecule will not approach a sphere to a distance smaller than Δ in order to avoid a loss of conformational entropy. For polymer molecules that are much larger than the colloidal spheres there is still an entropy loss, but this is substantially lower than that predicted by the Vrij theory. The theory is thus only valid for relatively large spheres. Vrij [16] assumed that the attractive interparticle potential between two spherical colloidal particles with diameter σ_c, which behave as hard spheres toward one another, equals $-\Pi_p V_{\text{overlap}}$. In the range $\sigma_c < r < (\sigma_c + \sigma_p)$ the interaction potential then equals

$$U(r) = -\frac{1}{6}\pi(\sigma_c+\sigma_p)^3\left[1-\frac{3r}{2(\sigma_c+\sigma_p)}+\frac{r^3}{2(\sigma_c+\sigma_p)^3}\right] \times \frac{c_p RT}{M}, \tag{1}$$

where r is the distance between the centers of the colloidal spheres and $c_p RT/M$ represents the ideal osmotic pressure Π_p of a polymer solution with concentration c_p. We denote the minimum of the interaction potential at $r=\sigma_c$, $U(\sigma_c)$, as U_0, which can be expressed as

$$U_0 = -\frac{1}{6}\pi(\sigma_c+\sigma_p)^3\left[1-\frac{3}{2(1+\zeta)}+\frac{1}{2(1+\zeta)^3}\right]\frac{c_p RT}{M} \tag{2}$$

where $\zeta = \sigma_p/\sigma_c$. The radius of gyration of the polymer molecules R_g is a good measure for the depletion layer thickness $\Delta(\equiv\sigma_p/2)$. The depletion interaction potential $U(r) = -\Pi_p V_{\text{overlap}}(r)$ is schematically drawn in Fig. 1(a) for $\zeta = 0.86$ as in the present study.

B. Adhesive hard sphere model

When an EPS is added to skim milk the casein micelles experience an effective attraction. A simple approach then is to use the adhesive hard sphere (AHS) model as introduced by Baxter [17]. Although this approach is less elegant than the Vrij theory, we will introduce it in order to study transport properties. In that way we can make a connection between dynamic light scattering (DLS) experiments and the attraction between colloidal particles, as will be shown in Sec. II C 1.

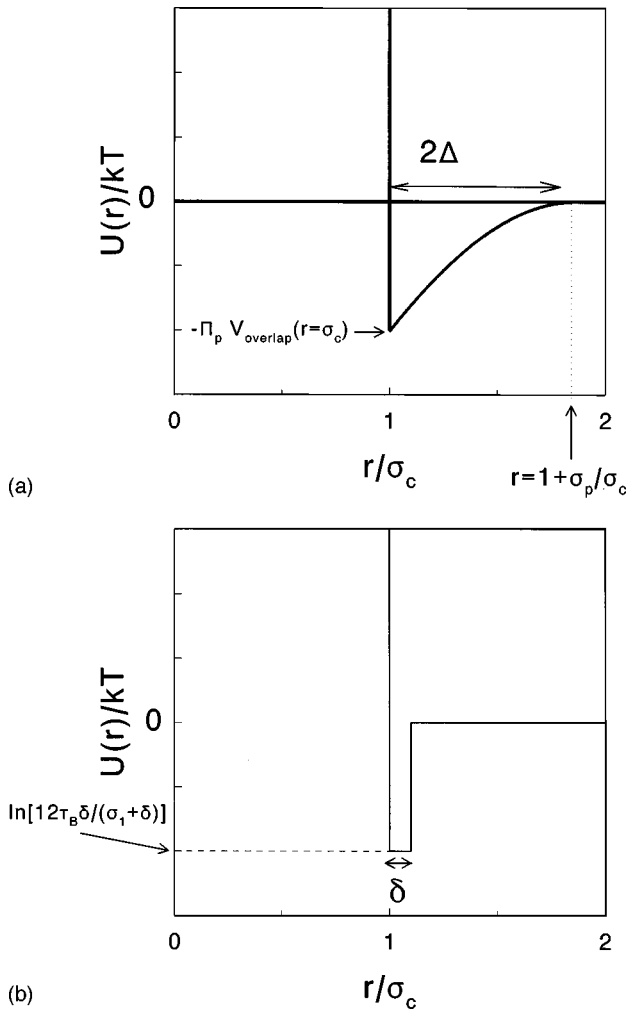

FIG. 1. Interaction potential profile for depletion interaction (a) following Vrij's theory [Eq. (1)] and for the adhesive hard sphere model (AHS) according to Eq. (3) (b).

For attractive spheres, for mathematical reasons Baxter [17] introduced a square well potential with an infinitely narrow width ($\lim \delta \to 0$, where δ is the range of the attraction) which is described in the equation

$$\frac{U(r)}{k_B T} = \begin{cases} +\infty, & 0 < r < \sigma_c \\ \ln[12\tau_B\delta/(\sigma_c+\delta)], & \sigma_c \leqslant r \leqslant (\sigma_c+\delta) \\ 0, & r > (\sigma_c+\delta), \end{cases} \tag{3}$$

where τ_B is the Baxter parameter, which is allowed to take values $0 < \tau_B < \infty$, and the inverse of τ_B reflects the strength of the attractive force (adhesiveness) between the spheres. The product $\tau_B\delta$ remains finite. A sketch of the AHS interaction potential is given in Fig. 1(b). It should be remarked here that the attractive potential induced by the EPS is certainly not short-range. The range of the potential, its width, is of the order of the radius of gyration of the EPS. Nevertheless we apply the Baxter model since it provides a simple theoretical framework which allows us to relate interaction

strength to dynamic light scattering. In experimental techniques like osmotic pressure and scattering measurements one measures the second virial coefficient B_2. In fact B_2 is simply related to τ_B by [18]:

$$B_2 = 4 - \frac{1}{\tau_B}. \tag{4}$$

Hence, the Baxter parameter can easily be obtained via B_2, and it has been shown that the Baxter parameter τ_B can be determined experimentally by dynamic light scattering [15], as will be discussed in Sec. II C.

C. Scattering techniques

1. Dynamic light scattering

With this technique the short-time self-diffusion coefficients can be measured, in our case of casein micelles as a function of the EPS concentration. Self-diffusion is related to the dynamics of a single particle in a system with a homogeneous density. In dilute colloidal suspensions containing spherical particles, the hydrodynamic radius of the diffusing sphere a_H can be calculated from the short time self-diffusion coefficient D_s through the Stokes-Einstein equation

$$D_s = \frac{k_B T}{6\pi\eta_s a_H}, \tag{5}$$

where η_s is the solvent viscosity. The parameter D_s depends on the particle volume fraction ϕ:

$$\frac{D_s}{D_0} = 1 - k_1\phi. \tag{6}$$

Here D_0 is the diffusion coefficient at infinite dilution and k_1 has a positive value. For a suspension of colloidal hard spheres Batchelor [19] and Felderhof [20] calculated the coefficient k_1 assuming that the diffusing particle is surrounded by nonadhesive Brownian hard spheres with fixed positions. They found $k_1 = 1.832$ [20]. When the particles become adhesive, the probability of of two particles being near one another is larger than for hard spheres, which leads to a stronger hydrodynamic interaction and friction. The equivalent Stokes radius appears to be increased. Cichocki and Felderhof [21] extended the equations of motions of Felderhof [20] to those for adhesive spheres, and their result for the diffusion coefficient is

$$\frac{D_s}{D_0} = 1 - \left(1.832 + \frac{0.295}{\tau_B}\right)\phi, \tag{7}$$

which shows that D_s decreases with increasing adhesiveness (τ_B becoming smaller). By measuring D_s Eq. (7) allows a calculation of τ_B for adhesive hard spheres. In a colloidal suspension of skim milk with casein micelles Π_p is larger at higher EPS concentration. This means that at higher EPS concentration the adhesiveness increases when the concentration of nonadsorbing EPS increases.

2. SANS

Neutrons can be regarded as electromagnetic waves and therefore neutron scattering is described here by the Rayleigh-Gans-Debye theory [22]. In a small-angle neutron scattering (SANS) experiment the normalized scattering intensity is then given by the Rayleigh ratio $R_\theta(Q)$, which depends on the wave vector Q which is defined as $4\pi n \sin(\theta/2)/\lambda_0$, where n is the refractive index, θ is the angle at which the scattered intensity is detected, and λ_0 is the wavelength in vacuo. For homodisperse sols $R_\theta(Q)$ is related to the structure factor $S(Q)$ and the scattering particle form factor $P(Q)$ by [22]

$$R_\theta(Q) = KcMP(Q)S(Q) \tag{8}$$

where c represents the particle concentration, M the molar mass of the particle, and K is a material constant which for SANS depends on the difference between the scattering length densities of particle and solvent. For colloidal spheres, the scattering form factor reads:

$$P(Q) = \left\{ 3\left(\frac{\sin(Qa) - Qa\cos(Qa)}{(Qa)^3} \right) \right\}^2 \tag{9}$$

with the sphere radius $a = \sigma_c/2$.

Upon adding nonadsorbing but ''invisible'' (i.e., with negligible contribution to the scattering) polymer molecules to a colloidal suspension, the scattering intensity will change. This originates from the fact that the structure of a colloidal suspension, which is measured via $S(Q)$, is strongly affected by the interactions between colloidal particles.

In the limit $Q = 0$, the structure factor is related to the isothermal osmotic compressibility $\partial\rho/\partial\Pi_c$ by

$$S(Q=0) = k_B T \frac{\partial\rho}{\partial\Pi_c}. \tag{10}$$

Here $\rho(=6\phi/\pi\sigma_c)$ is the number density, and Π_c is the osmotic pressure of the colloidal particles. For attractive particles $\partial\Pi_c/\partial\rho$ is smaller than for hard spheres and when $\partial\Pi_c/\partial\rho < 0$ the system spontaneously phase separates. At the spinodal the compressibility is infinite, the system shows critical opalescence, and $S^{-1}(Q=0) = 0$. This illustrates that $S(Q)$ is indicative of the stability of colloidal suspensions. Physically, this can be understood since $S(Q)$ is the Fourier transform of the radial distribution function $g(r)$ of the particles:

$$S(Q) = 1 + 4\pi\rho \int_0^\infty r^2 (g(r) - 1) \frac{\sin(Qr)}{Qr} dr, \tag{11}$$

where r is the distance from the center of a probe particle to the center of any random particle. The radial distribution function $g(r)$ reflects the probability of finding a particle at a distance r from the center of another particle. It is obvious that $g(r)$ changes when either the particle concentration or the particle interactions are changed. The radial distribution function is expressed in direct and indirect contributions by the Ornstein-Zernike equation (OZE) [23]

$$h(r)=c(r)+\rho\int c(r_{13})h(r_{23})dr_3, \tag{12}$$

where $c(r)$ is the direct correlation function, and $h(r)\equiv g(r)-1$ the total correlation function. The total correlation function is the sum of the direct correlation of particle 1 with particle 2 and an indirect correlation between 1 on 2 in which all other particles are involved. The total and direct correlation functions can be calculated if an appropriate closure relation is used.

For adhesive hard spheres, interacting via a Baxter potential, the authors of Ref. [24] solved the Ornstein-Zernike relation using the Percus-Yevick closure [25]. The $S(Q)$ obtained from the model of Ref. [24] closely matches the results of Kranendonk and Frenkel [26], who used computer simulations to calculate $S(Q)s$ of suspensions containing adhesive hard spheres.

We are interested in expressions for $S(Q)$ for colloidal suspensions with added nonadsorbing polymer. For any interaction potential Gillan [27] developed a solution procedure of the OZE with the hypernetted chain closure [28,29] defined by

$$c(r)=h(r)-\ln(g(r))-U(r)/k_BT. \tag{13}$$

Gillan's method combines the Picard method and the Newton-Raphson technique [27]. We apply the interaction potential profile suggested by Vrij [16] to Eqs. (12) and (13) and calculate $S(Q)$.

3. Turbidity measurement

The turbidity (τ) reflects the attenuation of a light beam by scattering when it passes through a sample. It is related to the transmission t by the Lambert-Beer relation

$$\tau=\frac{1}{b}\ln\left[\frac{1}{t}\right], \tag{14}$$

where b is the path length through the sample. If absorption of radiation can be neglected, so that all the reduction of the measured transmission is caused by scattering, a simple conservation law relates scattering and turbidity,

$$\tau(\lambda_0)=2\pi\int_0^{\pi}R_{\theta}(Q)\sin(\theta)d\theta \tag{15}$$

or, upon substituting Eq. (8) and $Q=4\pi n\sin(\theta/2)/\lambda_0$,

$$\tau(\lambda_0)=8\pi KcM\int_0^{4\pi n/\lambda_0}P(Q)S(Q)\left\{1+\left(1-2Q^2\left(\frac{\lambda_0}{4\pi n}\right)^2\right)^2\right\}Q\left(\frac{\lambda_0}{4\pi n}\right)^2dQ. \tag{16}$$

Since we can calculate $S(Q)$ as shown in Sec. II C 2, and take Eq. (9) for $P(Q)$, we can calculate the turbidity from Eq. (16).

III. EXPERIMENTAL METHODS

A. Material

An EPS was produced on a pilot-plant scale at NIZO [7]. A *Lactococcus lactis* subsp. *cremoris* NIZO B40 was used to inoculate a whey permeate medium. After production an EPS was isolated using various filtration steps [7]. This isolate was freeze dried and used as such in this study.

Reconstituted skim milk was prepared by mixing 10.45 g of skim milk powder in 100 g of demineralized water at 40 °C. The suspension was stirred and kept at this temperature for 45 min. Afterwards, the milk was centrifuged at 10^4 rpm for 20 min in order to remove the small amount of undissolved milk powder left in the solution. Measurements of the relative viscosity as a function of the casein micelle concentration by Jeurnink and De Kruif [30] showed that casein micelles can be considered as hard spheres and have a volume fraction of 0.130 in (low-heat) skim milk. Skim milk permeate (i.e., the ''solvent'' of the casein micelles) was prepared from skim milk by a membrane filtration process. An Amicon hollow-cartridge HIMPO 1-43 membrane with a cutoff of 0.1 μm was used. The pH of the permeate was the same as that of the skim milk (6.60 ± 0.10). The mixtures were prepared by dissolving the EPS in permeate and mixing this EPS–skim milk permeate solution with skim milk. All mixtures were studied at 298 K.

For the SANS measurements 99.9% D_2O (Sigma) was used to dissolve skim milk powder and the EPS. The pH, as measured with a pH meter, of the D_2O mixtures was 6.75. The D_2O skim milk permeate was prepared from the D_2O milk by ultracentrifugation.

In order to prevent growth of micro-organisms during the experiments we added 0.02%(m/m) sodium ethylmercurithiosalicylate ($C_2H_5HgSC_6H_4COONa$ thiomersal, BDH Chemicals) to the mixtures which prevented any bacterial growth and subsequent pH changes. In the absence of the EPS, skim milk and permeate containing thiomersal were stable for months.

B. Scattering techniques

1. Dynamic light scattering

Dynamic light scattering experiments were performed to determine the diffusion coefficients of the casein micelles with Malvern Hi-C particle size analysis equipment, which operates in a backscattering mode. Under these conditions the scattering vector has its maximum value at the given wavelength. At this Q value $Q\sigma_c\gg1$, which means that self-diffusion will dominate collective diffusion for our setup. Measurements were made at 298 K.

2. Small-angle neutron scattering

The SANS experiments were performed by using cold thermal neutrons emitted from the core of the high-flux

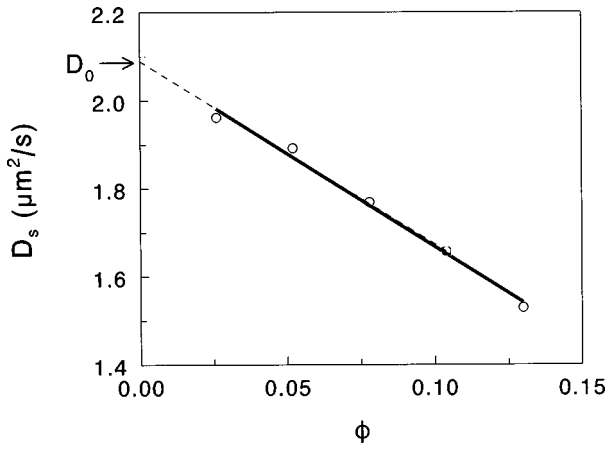

FIG. 2. The self-diffusion coefficient of casein micelles as a function of their volume fraction.

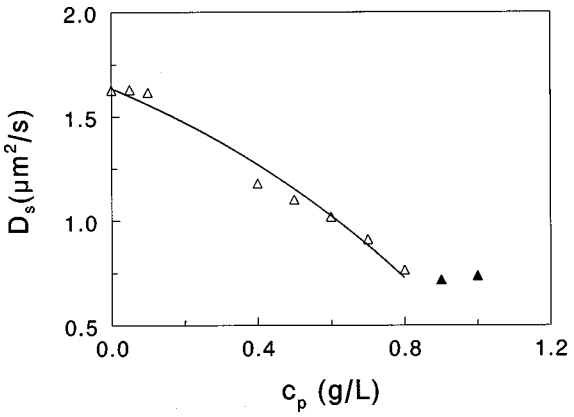

FIG. 3. Self-diffusion coefficients measured in diluted skim milk ($\phi=0.11$) as a function of the EPS concentration. Data points are given by the open triangles. The filled triangles represent samples within the two-phase region. The drawn curve was computed from Eqs. (7) and (17).

nuclear reactor at the Institute Max Von Laue–Paul Langevin in Grenoble (France) using the D-11 spectrometer, as described by lbel [31]. Hellma QS quartz cells were used with a sample path length of 2 mm. For this small path length multiple scattering is negligible at a volume fraction of 0.12 as studied. All samples were mixed thoroughly before measuring. For casein micelles, the $S(Q)$ peak, as calculated for a diameter of 200 nm, lies around $Q=0.031\,\mathrm{nm}^{-1}$. Therefore, we performed measurements in the range $0.01<Q<0.08\,\mathrm{nm}^{-1}$. In order to obtain the desired Q range, a sample-detector distance of 35.7 m was chosen. The mean wavelength of the emitted neutrons was 1.0 nm with a width at a half height of 9%.

3. Turbidity measurement

The experiments were made with a Hitachi (model U-1100) single beam spectrophotometer, and the samples were measured in quartz glass cuvettes (Hellma, type 110 QS). Cuvettes with a path length of 2 mm were chosen to enable an accurate measurement of the transmission. The light source of the spectrophotometer produces a wide range of radiation. The required wavelength can be selected by a prism or grating monochromator. The beam is split, and the beams are led to the sample cell and the reference cell (containing only permeate), respectively. The transmissions were measured by recording the intensities of sample (skim milk with or without an EPS) and permeate. To eliminate the effect of aggregated particles which may blur the results, the mixtures were filtered (pore size 5 μm) before use.

IV. RESULTS AND DISCUSSION

A. Self-diffusion

The diffusion coefficient of the casein micelles in milk and several solutions of milk diluted with permeate was measured in order to check whether the casein micelles behave as hard spheres. In Fig. 2 the self-diffusion coefficient (D_s) is shown as a function of the volume fraction of the casein micelles in permeate. This self-diffusion coefficient depends linearly on the volume fraction. By extrapolation to $\phi=0$, a value of $2.09\times10^{-12}\,\mathrm{m^2\,s^{-1}}$ was found for D_0. According to Eq. (5) this gives a hydrodynamic radius (a z average) of the casein micelles of 117 nm which is consistent with literature values [32,33] and with the distribution of casein micelles in skim milk from which a number-averaged radius of 100 nm follows [34]. The volume fraction dependence in permeate can be described with Eq. (6), with $k_1=2.0$, which is in reasonable agreement with the theoretical value of 1.83 for hard spheres.

The self-diffusion of the casein micelles was measured as a function of the EPS concentration. For $\phi=0.11$ the result is plotted in Fig. 3. The plotted curve was calculated from Eq. (7), using the following expression for the Baxter parameter τ_B:

$$\tau_B=\frac{\delta+\sigma_c}{12\delta}\exp\left(-\frac{V_{\mathrm{overlap}}(\sigma_c)c_p}{m}\right), \tag{17}$$

where $m=M/N_{AV}$ is the mass of a polymer molecule. This equation follows from combining Eqs. (1) and (3) and indicates how the attraction depends on the EPS concentration. The terms $(\delta+\sigma_c)/12\delta$ and $V_{\mathrm{overlap}}(\sigma_c)/m$ were used as fitting parameters. Equation (17) describes the measured data up to 0.8 g/L. For the two highest EPS concentrations, demixing was observed during the experiment and the diffusion coefficients of these samples were not fitted. It follows from Fig. 3 that increasing the EPS concentration gives a decrease in the self-diffusion coefficient which corresponds to a lower Baxter parameter and thus more attraction between the casein micelles. The Baxter result can be applied for short range attraction. It appears here that a qualitatively correct interpretation of the data can be given.

At very low EPS concentrations there is hardly any effect on the diffusion coefficient. If an EPS is adsorbed onto the casein micelles a thick layer (of order 80–90 nm, which is the radius of gyration) would form, which would strongly decrease the diffusion coefficient of the casein micelles: their hydrodynamic size would increase by a factor of about 1.7. The independence of D_s on c_p at very low concentrations indicates that indeed an EPS does not adsorb on the casein micelles. We found similar results at lower volume fractions of casein micelles.

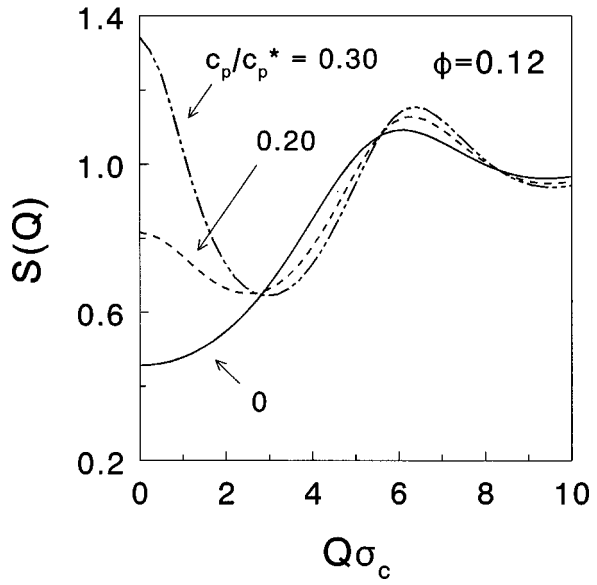

FIG. 4. The structure factor of hard sphere suspensions ($\phi = 0.12$) as a function of $Q\sigma_c$ for depletion interacting hard spheres with $\sigma_p/\sigma_c = 0.86$. Results are given for polymer concentrations of $c_p/c_p^* = 0$, 0.2, and 0.3.

B. Structure factors

In this section we compare SANS measurements with model calculations of structure factors as obtained from the theories given in Sec. II C 2. We have calculated $S(Q)$ as described in Sec. II C 2 from the depletion interaction potential as suggested by Vrij [16]. The $S(Q)$ profiles were calculated for a monodisperse suspension with a volume fraction of 0.12 without polymer molecules ($c_p = 0$), and in the presence of nonadsorbing polymer molecules ($\sigma_p = 176$ nm) at two concentrations $0.2c_p^*$ and $0.3c_p^*$, where $c_p^* = 3M/\{4\pi R_g^3 N_{AV}\}$ is the coil overlap concentration; it equals 0.9 ± 0.1 g/L for an EPS in a 0.10-M $NaNO_3$ aqueous solution. The results for $S(Q)$ are plotted in Fig. 4. At $Q\sigma_c = 2\pi$ we recover the characteristic first peak for the hard sphere suspension. Upon adding polymers the shape of the $S(Q)$ curve has significantly changed. At low Q, $S(Q)$ increases with increasing c_p, which corresponds to the fact that the system becomes less stable when the particles attract one another more strongly [for $1/S(Q=0) = 0$, spinodal decomposition is found].

From an experimental point of view it is convenient to normalize the structure factor. We have calculated $S(Q)/S(Q)_0$ by using the methods described in Sec. II C 2 for AHS and colloidal depletion interacting particles. We define $S(Q)_0$ as the structure factor of the hard sphere suspension, and take $S(Q)$ as the structure factor of the same suspension including attraction either by the AHS model or by depletion interaction. Results for calculated $S(Q)/S(Q)_0$ as a function of Q are given for colloidal particles with a diameter of 200 nm (casein micelles) in Figs. 5(a) (adhesive hard spheres) and 5(b) (depletion interaction). The results for both theoretical models are rather similar, showing that depletion interaction can be regarded as an effective attraction between the casein micelles. It is remarkable that for the broader depletion potential the oscillations are ''dampened'' more strongly and are of a ''shorter'' wavelength. Since the

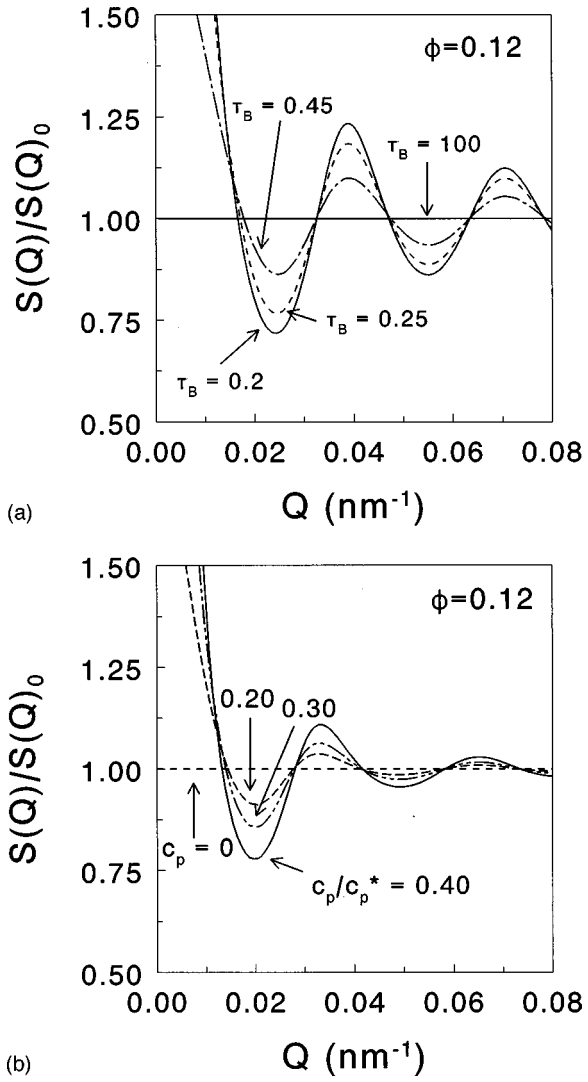

FIG. 5. Normalized structure factor as a function of Q for monodisperse particles with a diameter of 200 nm for (a) adhesive hard spheres for values of the Baxter parameter as indicated, and (b) for depletion interacting hard spheres at polymer concentrations as indicated.

depletion interaction calculations given in Fig. 5(b) are closer to the real system, we will compare these results with the experimental SANS results. For polydisperse systems the oscillations are progressively dampened with increasing Q, and only approximately the first minimum will still be visible. These polydisperity effects hardly affect $S(Q)$ in the low-Q range [35].

The scattering intensities were measured for skim milk in D_2O as well as for mixtures of EPS and skim milk in D_2O. The volume fraction of casein micelles was $\phi = 0.12$. The scattered intensity is plotted as a function of the wave vector in Fig. 6 for various EPS concentrations. By increasing the EPS concentration the scattering intensity decreased in the measured Q range. We have normalized the measured intensities $I(Q)$ with the intensity of skim milk without an EPS, $I(Q)_0$. In Fig. 7 the normalized scattered intensities $I(Q)/I(Q)_0$ are given as a function of Q for four EPS concentrations. We assume that the form factor of the casein micelles is not changed. Therefore changes in the scattered intensity are attributed to a change in $S(Q)$ and $I(Q)$

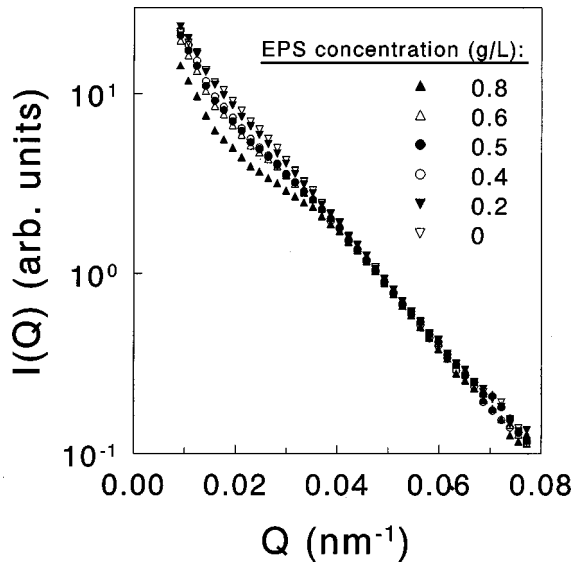

FIG. 6. The scattering intensity $I(Q)$ of skim milk–EPS mixtures as a function of Q as measured by SANS. The measured data are in a range from 0 to 0.8 g/L (EPS) are divided by the scattering intensity of the suspension ($\phi=0.12$) in the absence of an EPS.

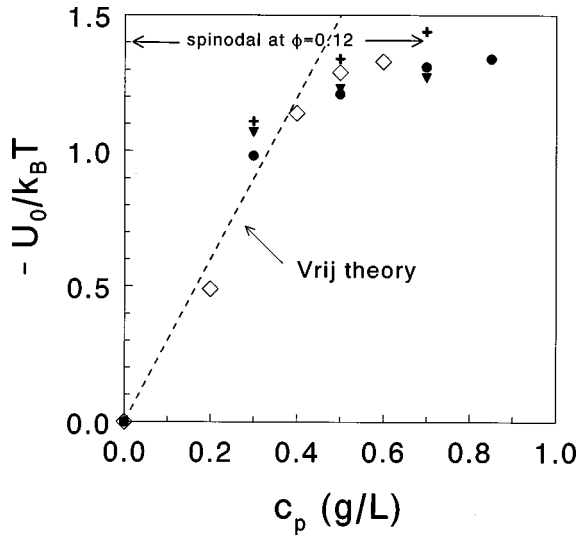

FIG. 8. The minimum of the interaction potential profile U_0/k_BT as a function of the EPS concentration c_p as calculated from the SANS measurements (open diamonds) and turbidity measurements (crosses for $\phi=0.06$, filled triangles for $\phi=0.08$, and filled circles for $\phi=0.10$).

$\sim S(Q)$. Then Eq. (8) can be rewritten as

$$\frac{I(Q)}{I(Q)_0}=\frac{S(Q)}{S(Q)_0}, \tag{18}$$

where $S(Q)_0$ is the structure factor of the suspension of casein micelles, and $S(Q)$ represents the structure factor of the same suspension when an EPS is added. From Fig. 7 it follows that $I(Q)/I(Q)_0$ has a minimum at $Q=0.02\,\mathrm{nm}^{-1}$. From Fig. 5(b) follows that $S(Q)/S(Q)_0$ is smaller than unity between $Q=0.013$ and $0.029\ \mathrm{nm}^{-1}$, and also goes through a minimum at $Q=0.02\,\mathrm{nm}^{-1}$. It is true that the experimental convex curve as given in Fig. 7 is wider than the theoretical one in Fig. 5(b). We think that this is mainly due to distribution in both micelle size and wavelength spread and divergence of the neutron beam, leading to a smearing out of the first $S(Q)$ peak.

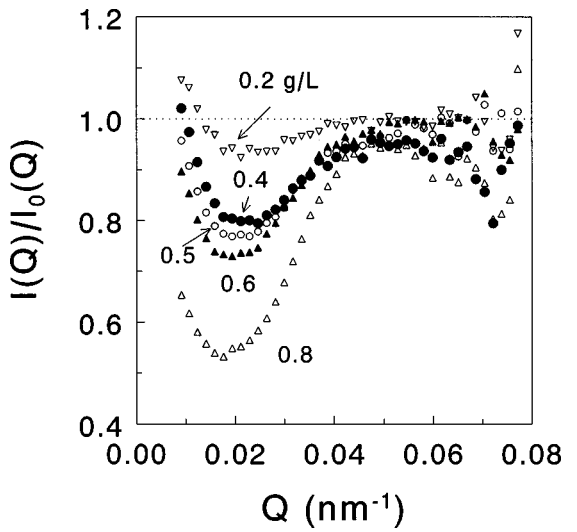

FIG. 7. The normalized scattering intensity $I(Q)/I(Q)_0$ of skim milk–EPS mixtures as a function of Q as measured by SANS. The measurements (in a range from 0.2 to 0.8 g/L EPS) are divided by the scattered intensity of the suspension ($\phi=0.12$) in the absence of an EPS.

The next step is a quantitative comparison between attractions as measured experimentally, presented in Fig. 7 and the prediction of the theory of Vrij. Therefore we calculated values for U_0 which gave the best correspondence of $S(Q)/S(Q)_0$ with the minimum of the $I(Q)/I(Q)_0$ curves. These U_0 values are plotted as a function of the experimental polymer concentration in Fig. 8. The prediction from the theory of Vrij as given by Eq. (1) is shown as a straight dotted curve. It is seen that the experimental data do not follow the straight curve as predicted by the Vrij theory, and that there is some discrepancy between the absolute values. This is probably due to the fact that the Vrij theory considers the chains as ideal and only applies for monodisperse polymers and spheres. The increase of U_0 with c_p, as found experimentally, has the shape of a saturation process; just before the spinodal is reached the increase in U_0 as a function of c_p is very small. Ye *et al.* [36] also calculated U_0 as a function of c_p from SANS for a depletion interacting colloidal dispersion, and found the same shape of the $U_0(c_p)$ curve. The position of the theoretical phase boundary expressed as U_0/k_BT is given by the arrow. From the experimental data we estimated the limiting polymer concentration as being 0.4–0.6 g/L, which corresponds with visual observation [37]. We conclude that experiment and theory are quite consistent for such a practical system. Information on the structure of a colloidal suspension can also be obtained from turbidity measurements, as presented in Sec. IV C.

C. Turbidity

First, we measured the transmission of permeate (with an EPS) and found that the EPS did not significantly affect the transmission in the range 400–750 nm over the relevant EPS concentrations. In this wavelength range absorption of pho-

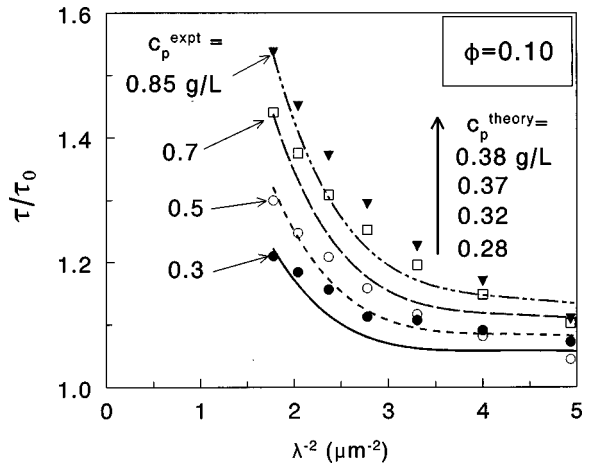

FIG. 9. Measured turbidities of skim milk with a volume fraction of micelles $\phi=0.10$ as a function of the inverse wavelength for various concentrations of EPS's, as indicated (c_p^{exp}). Best theoretical predictions of the Vrij model are given as (dashed) lines, and the polymer concentrations are indicated by c_p^{theory} (increasing from bottom to top).

ton energy can be considered to be absent in our system. Next we measured the transmission of skim milk with various amounts of EPS. Adding an EPS significantly increased the turbidity of skim milk suspensions at wavelengths larger than 500 nm, which was attributed to a depletion interaction between the casein micelles induced by the EPS.

The effect can be visualized clearly by dividing the turbidity of the mixture of the EPS and casein micelles by the turbidity of skim milk (only casein micelles). Any deviation from one should originate from interactions since the EPS's have a negligible scattering relative to the casein micelles. The turbidity of skim milk is indicated by the symbol τ_0.

Theoretical predictions were obtained from the Vrij theory by calculating the structure factor as described in Sec. II C 2 and integrating the resulting $S(Q)$ by applying Eq. (16). In Fig. 9 the theoretical results (curves) of the turbidity are plotted as a function of λ^{-2} as calculated from Eq. (16) for $\phi=0.10$, $\sigma_c=200$ nm, and $\zeta=0.86$. The refractive index of skim milk permeate at 25 °C was taken as 1.3475 [38], which is hardly affected by the EPS present and is close to the value for the refractive index of water at 25 °C. We chose λ^{-2} as a variable, since expansion of τ leads to a first-order λ^{-2} dependence [39]. For high values of λ^{-2} [corresponding to integration of $P(Q)S(Q)$ from 0 to high Q^2], τ/τ_0 approaches unity while for lower λ^{-2} values there is a characteristic upswing of τ/τ_0. This upswing originates from an increase of the structure factor. The upswing is stronger for higher polymer concentrations (more attraction). The line given for $c_p=0.38$ g/L is just below the theoretical spinodal.

The turbidity was measured as a function of wavelength at four EPS concentrations, 0.3, 0.5, 0.7, and 0.85 g/L for $\phi=0.06$, 0.08, and 0.10. The results for $\phi=0.10$ are given in Fig. 9. The experimental data qualitatively correspond very well to the theoretical predictions. The agreement is especially good in the range of the upswing at low λ^{-2}.

At high λ^{-2} values the experimental results for the various EPS concentrations seem to approach unity more rapidly (at lower λ^{-2} values) than the theoretical curves predict. This can be explained by a polydispersity effect [35]. Polydispersity gives rise to a dampened $S(Q)$ becoming unity for small wavelengths, which explains a faster decrease to unity of the experimental τ/τ_0 with decreasing wavelength. In general both experiment and theory show that upon increasing the EPS concentration the turbidity increases at long wavelengths which corresponds to a stronger attraction between the casein micelles. Quantitatively, the experimental and theoretical polymer concentrations have the same order of magnitude but differ by approximately a factor 2. This is due to the polydispersity of casein micelles, EPS's, and wavelength, and due to the limitations of the Vrij theory which applies only for ideal chains and does not take into account higher order terms in the osmotic pressure of the polymer solution.

The same turbidity experiments were done for $\phi=0.06$ and 0.08 with varying EPS concentrations. The main trends are the same as in Fig. 9. From the comparison with the model calculations we obtained the results given in Fig. 8 together with the SANS data. It follows that the depth of the potential well U_0 increases with increasing EPS concentration, and is quantitatively consistent with results from the SANS measurements.

V. CONCLUSIONS

Dynamic light scattering experiments, small-angle neutron scattering and turbidity measurements showed that the casein micelles become attractive upon adding an EPS. The attraction can be attributed to depletion interaction. The self-diffusion coefficients obtained from DLS can be interpreted by the adhesive sphere model. The attraction found by SANS and turbidity measurements can be described by the structure factors calculated from a theory based on the depletion interaction potential as described by the Vrij model. These findings show that mixing certain biopolymers together strongly affects the properties of the system, and that the calculation of the attraction can be used to obtain an idea of the resulting structure and consistency. The attractions not only affect the phase behavior but also the equilibrium and transport properties, such as the self-diffusion and the viscosity.

ACKNOWLEDGMENTS

This work was supported financially by the Netherlands Association of Biotechnology Centers (ABON). Cyril Renaud and Blandine Oudin are thanked for performing self-diffusion and turbidity experiments, respectively, and for their pleasant cooperation. Professor M. A. Cohen Stuart and Professor G. J. Fleer, from the Laboratory for Physical Chemistry and Colloid Science at Wageningen University, are thanked for their critical readings of the manuscript. Dr. P. Zoon and Dr. S. P. F. M. Roefs from NIZO are thanked for stimulating discussions.

[1] P. A. Sandford, I. W. Cottrell, and D. J. Pettitt, Pure Appl. Chem. **56**, 879 (1984).
[2] J. Cerning, FEMS Microbiol. Rev. **87**, 113 (1990).
[3] M. E. van Marle, Ph.D. thesis Twente University, The Netherlands, 1998.
[4] M. Gruter, B. R. Leeflang, J. Kuiper, J. P. Kamerling, and J. F. G. Vliegenthart, Carbohydr. Res. **231**, 273 (1992).
[5] S. F. Osman, W. F. Fett, and R. L. Dudley, Carbohydr. Res. **265**, 319 (1994).
[6] G. W. Robijn, D. J. C. van den Berg, H. Haas, J. P. Kamerling, and J. F. G. Vliegenthart, Carbohydr. Res. **276**, 117 (1995).
[7] R. Tuinier, P. Zoon, C. Olieman, M. A. Cohen Stuart, G. J. Fleer, and C. G. de Kruif, Biopolymers **49**, 1 (1999).
[8] V. Ya. Grinberg and V. B. Tolstoguzov, Food Hydrocoll. **11**, 145 (1997).
[9] C. G. De Kruif, Langmuir **8**, 2932 (1992).
[10] M. G. Semenova, G. E. Pavloskaya, and V. B. Tolstoguzov, Food Hydrocoll. **4**, 469 (1991).
[11] S. Kasapis, E. R. Morris, I. Norton, and A. H. Clark, Carbohydr. Pol. **21**, 243 (1993); **21**, 249 (1993); **21**, 261 (1993); **21**, 269 (1993).
[12] S. Asakura and F. Oosawa, J. Chem. Phys. **22**, 1255 (1954); J. Polym. Sci. **33**, 183 (1958).
[13] *Observation and Simulation of Phase Transitions in Complex Fluids*, edited by M. Baus, L. F. Rull, and J-P. Ryckaert (Kluwer, Dordrecht, 1995).
[14] H. N. W. Lekkerkerker, W. C. K. Poon, P. N. Pusey, A. Stroobants, and P. B. Warren, Europhys. Lett. **20**, 559 (1992).
[15] C. G. De Kruif, J. W. Jansen, and A. Vrij, *Symposium of Complex Fluids*, edited by S. A. Safraw and N. A. Clark (Wiley, New York, 1987).
[16] A. Vrij, Pure Appl. Chem. **48**, 471 (1976).
[17] R. J. Baxter, J. Chem. Phys. **49**, 2770 (1968).
[18] D. A. McQuarrie, *Statistical Mechanics* (Harper & Row, New York, 1976).
[19] G. K. Batchelor, J. Fluid Mech. **74**, 1 (1976).
[20] B. U. Felderhof, J. Phys. A **11**, 929 (1978).
[21] B. Cichocki and B. U. Felderhof, J. Chem. Phys. **93**, 4427 (1990).
[22] M. Kerker, *Scattering of Light and other Electromagnetic Radiation* (Academic, New York 1969).
[23] L. S. Ornstein and F. Zernike, Proc. K. Ned. Akad. Wet. **17**, 793 (1914).
[24] S. V. G. Menon, C. Manohar, and K. Srinivasa Rao, J. Chem. Phys. **95**, 9186 (1991).
[25] J. K. Percus and G. J. Yevick, Phys. Rev. **110**, 1 (1958).
[26] W. G. T. Kranendonk and D. Frenkel, Mol. Phys. **64**, 403 (1988).
[27] M. J. Gillan, Mol. Phys. **38**, 1781 (1979).
[28] J. M. J. van Leeuwen, J. Groeneveld, and J. de Boer, Physica (Amsterdam) **25**, 792 (1959).
[29] T. Morita and K. Hiriokem, Prog. Theor. Phys. **23**, 1003 (1960).
[30] Th. J. M. Jeurnink and C. G. De Kruif, J. Dairy Res. **60**, 139 (1993).
[31] K. Ibel, J. Appl. Crystallogr. **9**, 296 (1976).
[32] R. Bauer, M. Hansen, L. Ogendal, S. B. Lomholt, and K. B. Qvist, J. Chem. Phys. **103**, 2725 (1995).
[33] S. Hansen, R. Bauer, S. B. Lomholt, K. B. Quist, J. S. Pedersen, and K. Mortensen, Eur. Biophys. J. **24**, 143 (1996).
[34] C. G. De Kruif, J. Dairy Sci. **81**, 3019 (1998).
[35] D. Frenkel, R. J. Vos, C. G. De Kruif, and A. Vrij, J. Chem. Phys. **84**, 4625 (1986).
[36] X. Ye, T. Narayahan, P. Tong, and J. S. Huang, Phys. Rev. Lett. **76**, 4640 (1996).
[37] R. Tuinier and C. G. de Kruif, J. Chem. Phys. **110**, 9296 (1999).
[38] P. Walstra and R. Jenness, *Dairy Chemistry and Physics* (Wiley, New York, 1984).
[39] M. H. G. M. Penders and A. Vrij, J. Chem. Phys. **93**, 3704 (1990).